

CONTACT ANGLE HYSTERESIS CHARACTERIZATION OF TEXTURED SUPER-HYDROPHOBIC SURFACES

Ashutosh Shastry, Shaghayegh Abbasi, Aziel Epilepsia, and Karl F. Böhringer

Department of Electrical Engineering, University of Washington, Seattle, Washington, USA

(Tel: +1-206-543-5218; E-mail: ashutosh@u.washington.edu)

Abstract: This paper presents the fabrication of rough super-hydrophobic surfaces, dynamic high-speed measurements of sliding angles of water droplets, and develops a mechanistic understanding of contact angle hysteresis—the major dissipative mechanism in droplet based microfluidic systems. We investigate texture-dependence of hysteresis, evaluate the current model, propose a modification, and observe that the two models—current and proposed—are useful bounds on hysteresis of the surface except in ultra-hydrophobic regime where observed hysteresis is significantly higher than predictions of either model.

Keywords: droplet microfluidics, super-hydrophobic surfaces, contact angle hysteresis

INTRODUCTION

Droplet based systems make temporally and spatially resolved chemistries possible—creating exciting possibilities for lab-on-chip assay. A droplet resting on a surface requires a threshold force to set it in motion. Contact angle hysteresis is a measure of this force of pinning of the three-phase contact line to the solid surface and is attributed to physical and chemical inhomogeneities [1]. For such digital microfluidic systems, it is desirable that the surfaces have a low force threshold to set the droplet in motion. Eventually, with enough force, the line breaks off and the droplet begins to move. For electrowetting based devices [2], low-hysteresis and low-drag surfaces [3] could make sub-CMOS actuation voltages possible—enabling totally integrated microfluidic platforms.

Textured superhydrophobic surfaces are promising candidates for digital microfluidic systems because of the relative ease with which the droplet can move on them. A sessile droplet on a textured superhydrophobic surface could either be conformal with the surface, resting in the “Wenzel” state or it could rest contacting the tops of asperities in the “Fakir” state [4]. Since the solid-liquid contact area in the Fakir state is low, it is worth exploring the hysteresis behavior of droplets in this state.

The apparent contact angles in the two states are given by Eq. 1 and Eq. 2 [4], where ϕ and r are

texture parameters explained in Fig. 1 and θ_i is the equilibrium contact angle of the smooth surface.

$$\theta_W = r \cos \theta_i \quad (1)$$

$$\theta_F = -1 + \phi(1 + \cos \theta_i) \quad (2)$$

There has been a renewed interest in understanding contact angle hysteresis behavior of these surfaces. He et al. [5] performed dynamic measurements on sliding droplets, modeled the receding angle using Fort and Roura’s approach of trailing water film [6] for receding angles and a heuristic model for the advancing angle.

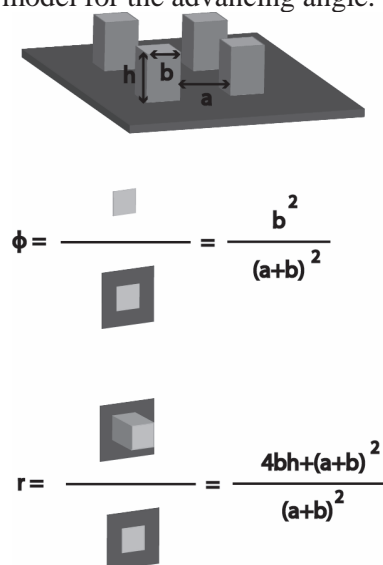


Figure 1: The texture parameters ϕ and r are expressed in terms of the design parameters a (gap length), b (pillar size) and h (pillar height), where ϕ is the fraction of pillar top area over total horizontal surface area and r is the fraction of total surface area over total horizontal surface area.

Understanding the quantitative relationship between the impeding force of contact angle hysteresis and surface parameters is therefore an important milestone—the one pursued in this work.

MATERIALS AND METHODS

We built rough surfaces realized by pillars of controlled geometry in silicon. Mask layouts were made using L-Edit®, and transparency masks were used for photolithography of 4" <100> silicon wafers with AZ4620 resist. Pillars were etched using standard Bosch® process for deep reactive ion etching (DRIE). Finally, hydrophobic coating of fluorinated-octyl-trichloro-silane (FOTS) was deposited by CVD on piranha activated silicon surface [8]. The fabrication process is detailed in Fig. 2.

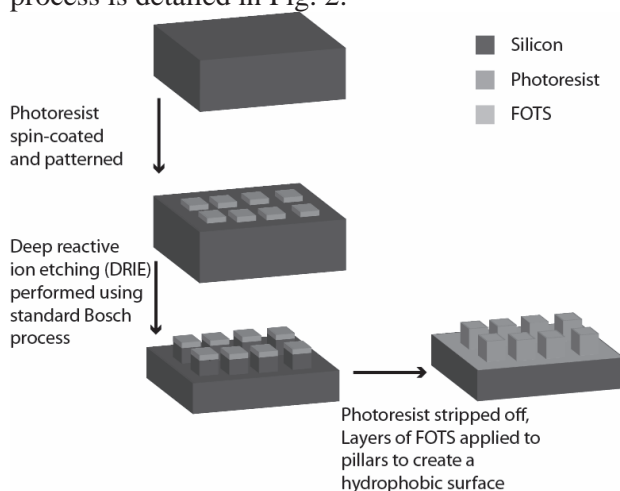


Figure 2: Fabrication Process: Lithography using AZ4620 followed by DRIE using Bosch® process to create the pillars in silicon. Si surface is activated by piranha treatment and chemical vapor deposition of fluorinated-octyl-trichlorosilane (FOTS) is carried out to complete the fabrication of test surfaces.

The test surfaces were mounted on the goniometer stage and droplets of measured volumes were deposited on them ensuring Fakir state where the droplet rests on pillar tops.

These droplets were expanded and contracted using a computer controlled syringe pump as shown in Fig. 3. A video was recorded and contact

angles were measured on individual frames. In our earlier work [5], we had reported a statistical method of obtaining dynamic angles. In this work we obtain direct measurements from the moving edge, overcoming aliasing errors, using high speed camera recordings at 250 fps.

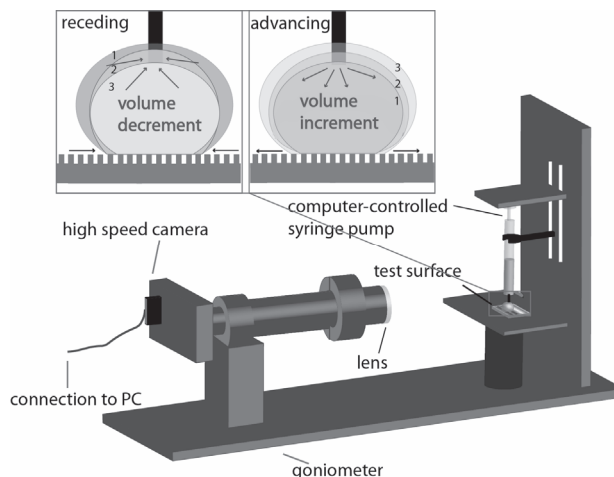


Figure 3: Goniometer setup explaining advancing and receding contact angle measurements. The needle of the syringe pump is immersed in the droplet and volume is added or subtracted.

RESULTS AND DISCUSSION

Fig. 4(a) shows the moving edge and Fig. 4(b) reports advancing angle from 32 ms before the edge “rolls over” to the next pillar. Advancing angle increases as the droplet volume increases but drops sharply as the advancing edge moves from one pillar to another—thereby increasing the droplet footprint and relaxing the liquid-vapor interface. Since advancing edge rolled over, we expect the advancing angle to be close to $\sim 180^\circ$ —independent of pillar dimensions and spacing.

Similar measurements were carried out for the “sliding” receding edge. Fig 5(a) shows the receding edge. The receding angle keeps decreasing till the edge snaps off the pillar top surface and attaches to the next pillar. This step increase in receding angle is captured in Fig. 5(b). Since the sliding edge is pinned to the pillar top surfaces, we expected this pinning—captured by $\cos\theta_R$ —to decrease as ϕ decreased. Movies were made for surfaces of varying texture— ϕ ranging from 0.025 to 0.9—and the data was plotted.

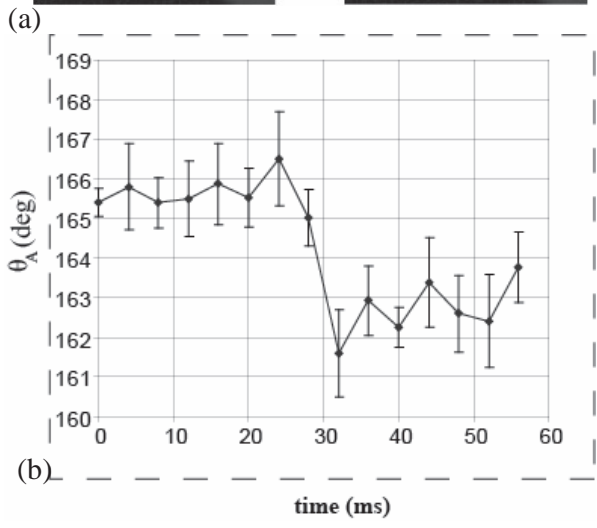
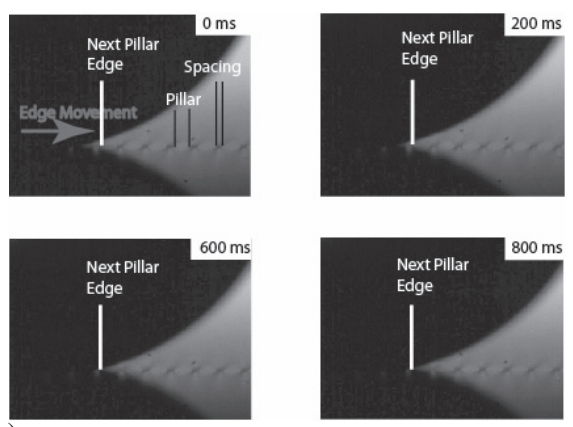


Figure 4: Advancing Angle Measurements: (a) Four frames show the landing of the advancing edge. (b) A plot of advancing angle eight frames before and after landing helps determine the maximum advancing contact angle. For every surface, the mean from three such recordings is used to determine the characteristic advancing angle.

The cosines of advancing angles were virtually invariant as seen in Fig. 6. This is distinct from the current advancing angle model given in Eq. 3, which is a heuristic relation due to He et al. [6].

$$\cos\theta_A = -1 + \phi(1 + \cos\theta_{i,A}) \quad (3)$$

We observe in Fig. 6 that this model underestimates advancing angle hysteresis. Our observations validate the “rolling” mechanism—the advancing angle is indeed insensitive to texture and stays virtually constant at ~168°.

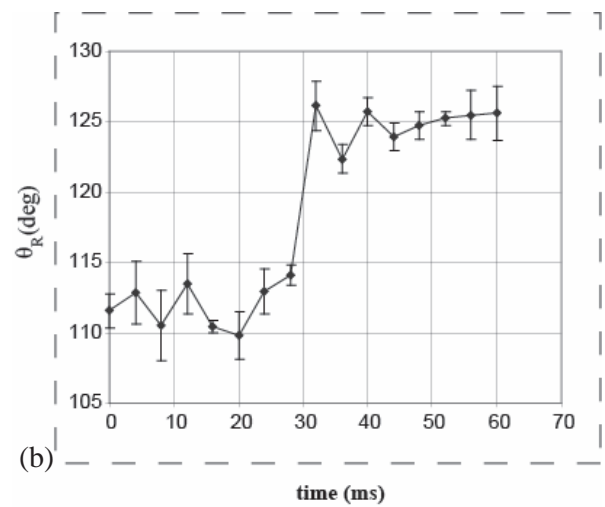
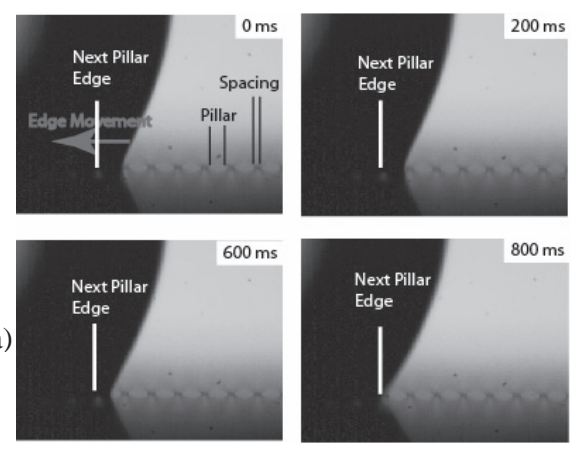


Figure 5: Receding Angle Measurements: (a) Four frames show the snapping of the receding edge. (b) A plot of receding angle eight frames before and after snapping helps determine the minimum receding contact angle. For every surface, the mean from three such recordings is used to determine the characteristic receding angle.

The cosines of receding angles decreased linearly with decreasing ϕ (Fig. 7). We believe that “sliding” as opposed to “rolling” is the reason why receding angle is far more sensitive to texture than the advancing angle as evident by comparing Fig. 6 and Fig. 7.

The current model for receding angle due to He et al. [6] is given in Eq. 4.

$$\cos\theta_R = 2\phi - 1 \quad (4)$$

It is obtained assuming a complete film left behind on the pillar tops [7]. Fig. 7 shows that, complete

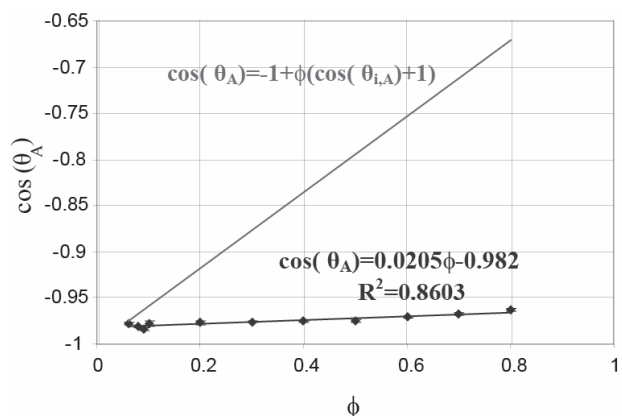


Figure 6: $\cos\theta_A$ versus ϕ for test surfaces with ϕ ranging from 0.05 to 0.9. Experimental data is plotted along with model predictions.

film, originally for hydrophilic surfaces [7], overestimates receding angle hysteresis to provide an upper bound (for $\phi > 0.1$). We re-derived the relation to obtain Eq. 5—hypothesizing “partial” coverage of pillar tops by the trailing film.

$$\cos \theta_R = \phi (f+1) - 1 \quad (5)$$

where “ f ” is the fraction of pillar tops covered by the trailing film. We further propose that “ $f = 0$ ” provides the lower bound to hysteresis—there is hysteresis because of texture even if no film is left behind.

Substituting for f into Eq. 5 we obtain Eq. 6, which is our proposed model for the receding angle.

$$\cos \theta_R = \phi - 1 \quad (6)$$

We observe in Fig. 7 that our model provides a lower bound to hysteresis. For ultra-hydrophobic surfaces ($\phi < 0.1$), however, hysteresis is higher than either model prediction. We postulate that it is pinning of the droplet edge by the pillar edges and not the solid-liquid area fraction ϕ that controls the hysteresis behavior in this regime. Work is in progress to develop that hypothesis [8].

CONCLUSION

This work marks an important step towards engineering droplet behavior on textured superhydrophobic surfaces by identifying critical trends that will shape the design rules for minimal hysteresis surfaces optimal for droplet actuation.

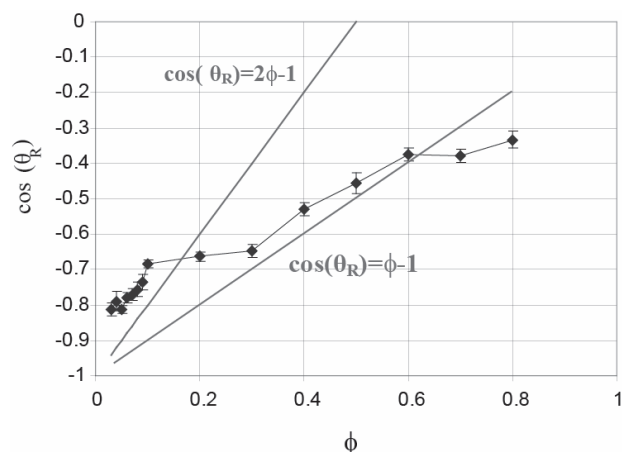


Figure 7: a) Entire range of ϕ : $\cos\theta_R$ versus ϕ for surfaces with ϕ values ranging from 0.01 to 0.9. Experimental data is plotted along with predictions from current and our area models.

ACKNOWLEDGEMENTS

This work is funded by NIH Center of Excellence in Genomic Science and Technology grant 1-P50-HG002360-01.

REFERENCES:

- [1] Pierre-Gilles de Gennes, F. Brochard-Wyart, D. Quere. *Capillarity and Wetting Phenomena: Drops, Bubbles, Pearls, Waves*, Springer-Verlag Inc., New York, 2004.
- [2] F. Mugele and J.-C. Baret, *J. Phys. :Cond. Mat.*, vol. 17, pp. R705–R774, 2005.
- [3] C. Cottin-Bizonne, J.-L. Barrat, L. Bocquet, and E. Charlaix, *Nat. Mat.*, vol. 2, pp.237240, 2003.
- [4] A. Lafuma and D. Quéré, *Nat. Mat.*, vol.2, pp. 457–460, 2003.
- [5] A. Shastry, A. Epilepsia, M. Case, S. Abbasi and K. F. Böhringer, In Proc. of *MicroTAS*, pp. 122-124, Nov. 2006, Tokyo, Japan
- [6] B. He, J. Lee, and N. A. Patankar, *Coll. Surf. A: Phys. Eng. Asp.*, vol. 248, pp. 101–104, 2004.
- [7] P. Roura and J. Fort, *Phys. Rev. E*, vol. 64, no. 011601, pp. 1–5, 2001.
- [8] A. Shastry, S. Abbasi and K.F. Böhringer, “Rolling and Sliding Fakir Drops Explain Contact Angle Hysteresis Behavior of Microtextured Superhydrophobic Surfaces”, submitted, 2007.